Terahertz vibration–rotation–tunneling spectroscopy of the propane–water dimer: The ortho-state of a 20 cm−1 torsion

ARTICLE *in* CHEMICAL PHYSICS LETTERS · SEPTEMBER 2014

Impact Factor: 1.9 · DOI: 10.1016/j.cplett.2014.08.019

Chemical Physics Letters 612 (2014) 167–171

Contents lists available at ScienceDirect

Chemical Physics Letters

journal homepage: www.elsevier.com/locate/cplett

Terahertz vibration-rotation-tunneling spectroscopy of the propane–water dimer: The *ortho*-state of a 20 cm^{-1} torsion

Wei Lin[a], David W. Steyert[b], Nikolaus C. Hlavacek[b], Anamika Mukhopadhyay[b], Ralph H. Page[b], Peter H. Siegel[c], Richard J. Saykally[b,*]

[a] Department of Chemistry and Environmental Sciences, University of Texas at Brownsville, One West University Blvd., Brownsville, TX 78520, United States
[b] Department of Chemistry, University of California, Berkeley, CA 94720, United States
[c] Department of Electrical Engineering, Caltech, Pasadena, CA 91125, United States

ARTICLE INFO

Article history:
Received 21 July 2014
In final form 7 August 2014
Available online 14 August 2014

ABSTRACT

We report the detailed characterization of a torsional vibration-rotation-tunneling band of the *ortho*-state of the propane–water dimer in the spectral region near 20 cm^{-1} (0.6 THz). This work extends the previously reported studies with more than one hundred new transitions included in a combined fit with the 155 previously reported transitions in both the microwave and terahertz regions for this torsional band. More than six hundred transitions have now been recorded in the interval 500 and 810 GHz.

1. Introduction

Terrestrial clathrate hydrates are envisioned as a potentially major energy source of the future [1], and may be an important factor in both past and future climate change [2]. The detailed composition of natural-gas clathrates is quite variable; methane is always the dominant hydrocarbon component, but ethane, propane, and butane are also abundant (in the 1–10% range). The presence of these higher hydrocarbons engenders greater stability for natural gas clathrate hydrates relative to pure methane clathrates [3], clearly an important consideration for designing schemes to extract clathrates from their extreme geological environments [1]. Computer simulations of clathrate stability and decomposition pathways are an essential component of this scenario, and these require accurate potential-surface models for describing the interactions among water and hydrocarbon molecules. Precise spectroscopic measurements of the intermolecular vibration-rotation-tunneling (VRT) states of gaseous water-hydrocarbon clusters, particularly the dimers, provide an important route to developing and calibrating such potential models, as has been demonstrated for the case of pure-water models [4,5,6].

Water–hydrocarbon interactions are important in another context, viz. elucidating the details of 'hydrophobic effects' [7]. In the case of water–methane interactions, we have shown [8] that the repulsive wall of the pairwise interaction potential directs the OH bond of water into the threefold hollow of the methyl group, thereby facilitating closest approach of the molecules. Other studies support this conclusion [9,10,11,12]. Extending this picture to higher hydrocarbons is a goal of our ongoing work, and this letter continues that effort.

We have published the results of previous studies of the propane–water dimer by microwave and terahertz VRT spectroscopy [13,14]. In the latter work, we described the observation and partial characterization of a low-frequency torsional vibration. Here we extend this study to include 144 additional transitions near 20 cm^{-1} involving this same torsional state. From analysis of the spectra, we deduce that the excited state of this torsional band is fairly rigid. There is no significant perturbation for the excited state, contrary to what we suggested earlier [18].

For the propane–water dimer, there are two low-lying states corresponding to the two nuclear spin states of water: the two spin ½ hydrogen nuclei can form two orientations (*ortho*- and *para*-) having a statistical weight ratio of 3:1, respectively. These two states can be interpreted as the result of water proton interchange tunneling. The direct measurement of the splitting between the two states is, however, hindered by electric-dipole selection rules forbidding nuclear spin flips. The previous microwave spectroscopy study of the propane–water dimer [13] unambiguously determined the rotational constants for both states from the intensities of the pure rotational transitions. Based on those results, we can assign the present band to propane–water dimer states correlating to the

* Corresponding author.
E-mail address: saykally@berkeley.edu (R.J. Saykally).

http://dx.doi.org/10.1016/j.cplett.2014.08.019
0009-2614/

ortho-state of water. In the current analysis, we included both the microwave and the VRT datasets in the same fit, with the proper statistical weights for the two types of measurements.

2. Experiment

Terahertz VRT spectra of the propane–water dimer were observed in a continuous supersonic planar jet expansion probed by a tunable far infrared (terahertz) laser spectrometer. The spectrometer has been described in detail elsewhere [15,16], so only a brief description is given here. The tunable terahertz radiation is generated by mixing the output from an optically pumped line-tunable far infrared gas laser with continuously tunable frequency-modulated microwaves using a Schottky barrier diode. Light is generated at the sum and difference frequencies ($\upsilon = \upsilon_{FIR} \pm \upsilon_{MW}$). A Michelson polarizing interferometer is used to separate the tunable sideband radiation from the much stronger residual THz center frequency radiation. The sidebands are then directed to multipass optics that encompass the supersonic expansion of the target molecular system. This supersonic expansion, formed by expanding 1–2 atm of a 3% mixture of propane (instrument purity, 99.5%, flow rate 0.02 SSCFM, Matheson) in argon (99.995% pure, Liquid Air Corporation) bubbled through distilled water under a backing pressure of 1120 Torr through a $4'' \times 0.005''$ slit nozzle, creates a population of propane–water dimers with a temperature of about 4 K. After passing ~10 times through the expansion, the radiation is detected by a liquid helium-cooled detector (either a Rollins-mode indium antimonide detector or a Putley-mode indium antimonide detector). The far infrared laser lines used for this scan were 527.9260 GHz (DCOOD), 584.3882 GHz (HCOOH), 639.1846 GHz (CH_3OH), 692.9513 GHz (HCOOH), 716.1574 GHz (HCOOH), 761.6083 GHz (HCOOH), 768.8820 GHz (DCOOD), 787.7555 GHz (DCOOD). The microwave frequency ranges were chosen so that the complete frequency range from 498 GHz to 810 GHz was covered. The Stark effect was used to help assign the complicated spectra [14]. The spectra carrier of each absorption line was checked by first turning off the propane flow while leaving the argon–water flow on and then vice versa. This check eliminated many transitions from the scan that do not depend on the propane (and are presumably due to argon–water clusters). Only the transitions that require both the propane flow and argon–water flow were kept in the dataset.

3. Observed spectra and analysis

A total of more than 600 transitions was recorded with ca. 2 MHz precision. 146 transitions were assigned to a *c*-type band involving the *ortho*-state of the propane–water dimer [14]. The initial assignment method was described previously in terms of using the Stark effect measurements and the lower/higher state combination-differences [14]. Clearly, many unassigned transitions remain in this region. In particular, there is a stack of $K_a = 2$–3 transitions wherein the measured frequencies are consistently lower by about 20 MHz than predicted. After reassigning the 512 616.5 MHz transition, rather than that at 512 635.8 MHz in Ref. [14], to the $7_{26} \leftarrow 8_{36}$ transition, we were able to add many transitions to the fit and refine the prediction for the $K_a = 3$–4 stack. After several iterations, we added more than one hundred transitions to the fit, while keeping rms error lower than the experimental error of several MHz. Figure 1 shows a stick spectrum of the previously 146 assigned transitions and of the 290 assigned transitions after this work. The added new transitions are listed in Table 1. These transitions have been least-squares fit together with the previous 146 THz-regime transitions and 9 microwave transitions in a weighted fit to the standard semi-rigid rotor Hamiltonian using SPFIT [17].

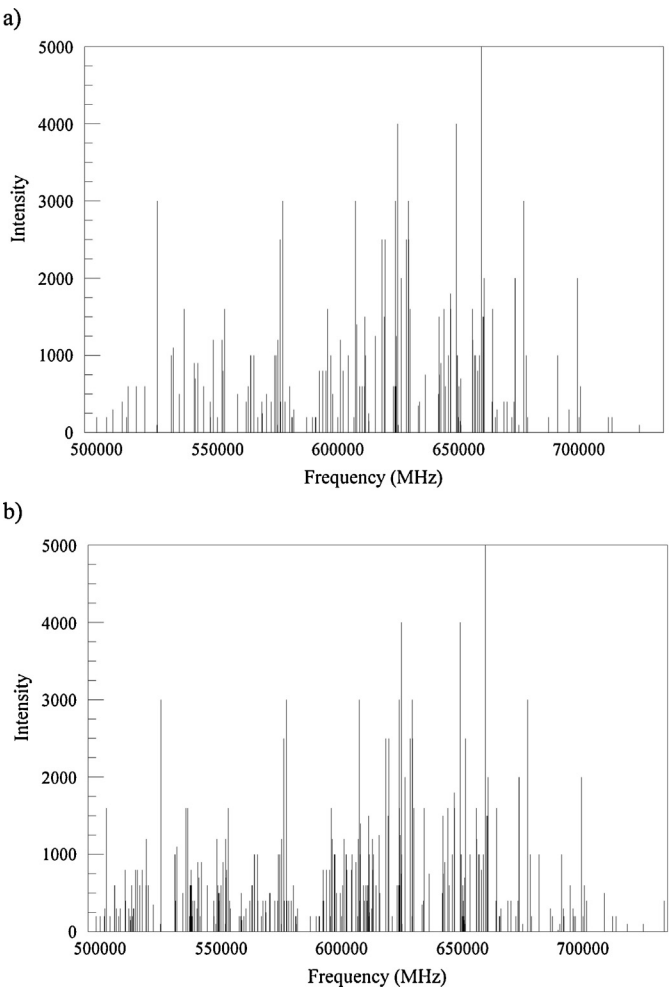

Figure 1. (a) Stick spectrum of the 146 assigned transitions from reference 14. (b) Stick spectrum of the 290 assigned transitions including the ones from Ref. [14] and the new transitions from this work. It should be noted that this is a composite spectrum, including transitions from five laser lines. Only the intensities of transitions recorded using a given laser line can be sensibly compared.

Table 2 lists the spectroscopic constants resulting from the fit, in comparison to the previous results. The transitions were fitted to an asymmetric top semi-rigid Hamiltonian with three rotational constants, five quartic centrifugal distortion constants, a few sextic centrifugal distortion constants for both the ground state and the excited state and the band origin of the excited state. As shown in Table 2, after adding the additional transitions to the fit, most of the rotational constants for the ground state and upper state remain near their previous values. These transitions, however, made it possible to precisely determine the important D_K value for the ground state for the first time. Some of the centrifugal distortion constants have also been significantly revised. It also clarified the origin of the >100 lines remaining in the same frequency region assigned for the torsional band. It is clear after the analysis presented here that the excited state of this torsional band is free from any large perturbation, unlike what had been suggested previously [18].

For most weakly bound dimers, the *a* inertial axis is aligned very closely with the line connecting the centers of mass of the two subunits. The *A* rotational constant of the *ortho*-propane–water dimer ground state was determined to be 8442.152 (62) MHz, whereas the *B* rotational constant of free propane was reported as 8446.07 MHz [19]. The fact that these two constants are so close indicates that

Table 1
Measured new frequencies for the *ortho*-state of the propane–water dimer.

$J'_{Ka',Kc'} \leftarrow J''_{Ka'',Kc''}$	Freq. MHz	Residual	$J'_{Ka',Kc'} \leftarrow J''_{Ka'',Kc''}$	Freq. MHz	Residual
$7_{0,7} \leftarrow 7_{1,7}$	579 112.7	0.9	$7_{3,5} \leftarrow 8_{4,5}$	501 685.3	0.3
$5_{0,5} \leftarrow 4_{1,3}$	592 614.8	0.8	$7_{3,4} \leftarrow 8_{4,4}$	501 897.1	−0.3
$6_{0,6} \leftarrow 5_{1,4}$	595 098.0	2.2	$6_{3,4} \leftarrow 7_{4,4}$	505 992.3	0.1
$7_{0,7} \leftarrow 6_{1,5}$	597 016.9	1.7	$6_{3,3} \leftarrow 7_{4,3}$	505 079.0	−0.8
$7_{1,6} \leftarrow 8_{0,8}$	562 961.5	1.2	$5_{3,3} \leftarrow 6_{4,3}$	510 308.7	−3.1
$5_{1,4} \leftarrow 6_{0,6}$	565 286.0	1.9	$4_{3,2} \leftarrow 5_{4,2}$	514 652.2	−0.5
$4_{1,3} \leftarrow 5_{0,5}$	567 431.3	−0.9	$4_{3,1} \leftarrow 5_{4,1}$	514 659.4	−0.9
$3_{1,2} \leftarrow 4_{0,4}$	570 203.8	−1.4	$3_{3,1} \leftarrow 4_{4,1}$	519 021.4	2.1
$2_{1,1} \leftarrow 3_{0,3}$	573 527.9	−0.3	$3_{3,0} \leftarrow 4_{4,0}$	519 021.4	1.0
$1_{1,0} \leftarrow 2_{0,2}$	577 310.2	−0.9	$4_{3,2} \leftarrow 4_{4,0}$	537 074.5	0.6
$2_{1,2} \leftarrow 2_{2,0}$	560 421.3	1.7	$4_{3,1} \leftarrow 4_{4,1}$	537 082.4	0.4
$3_{1,3} \leftarrow 3_{2,1}$	559 584.3	1.9	$5_{3,3} \leftarrow 5_{4,1}$	537 237.2	−2.3
$4_{1,4} \leftarrow 4_{2,2}$	558 305.3	0.6	$6_{3,4} \leftarrow 6_{4,2}$	537 437.7	1.2
$6_{1,6} \leftarrow 6_{2,4}$	553 968.9	0.5	$6_{3,3} \leftarrow 6_{4,3}$	537 534.4	0.4
$6_{1,5} \leftarrow 5_{2,3}$	592 253.4	1.8	$7_{3,5} \leftarrow 7_{4,3}$	537 655.9	1.8
$7_{1,6} \leftarrow 6_{2,4}$	597 267.1	2.2	$7_{3,4} \leftarrow 7_{4,4}$	537 898.3	0.9
$8_{1,7} \leftarrow 7_{2,5}$	601 874.2	1.5	$8_{3,6} \leftarrow 8_{4,4}$	537 874.6	2.3
$9_{1,8} \leftarrow 8_{2,6}$	605 967.7	1.9	$8_{3,5} \leftarrow 8_{4,5}$	538 404.8	0.5
$10_{1,9} \leftarrow 9_{2,7}$	609 462.8	−0.3	$9_{3,6} \leftarrow 9_{4,6}$	539 110.0	0.1
$11_{2,9} \leftarrow 12_{1,11}$	547 926.1	1.5	$10_{3,7} \leftarrow 10_{4,7}$	540 078.8	−0.5
$9_{2,7} \leftarrow 10_{1,9}$	551 806.8	−0.1	$11_{3,9} \leftarrow 11_{4,7}$	538 133.9	−1.4
$7_{2,5} \leftarrow 8_{1,7}$	558 710.9	0.8	$11_{3,8} \leftarrow 11_{4,8}$	541 377.2	−0.9
$6_{2,4} \leftarrow 7_{1,6}$	563 092.2	0.6	$13_{3,11} \leftarrow 13_{4,9}$	537 293.3	0.4
$2_{2,0} \leftarrow 2_{1,2}$	599 443.1	−0.9	$4_{4,0} \leftarrow 4_{3,2}$	624 189.1	1.1
$3_{2,1} \leftarrow 3_{1,3}$	600 467.7	1.2	$5_{4,1} \leftarrow 5_{3,3}$	624 277.8	0.1
$4_{2,2} \leftarrow 4_{1,4}$	601 980.6	0.8	$8_{4,4} \leftarrow 8_{3,6}$	624 664.6	1.6
$5_{2,3} \leftarrow 5_{1,5}$	604 091.2	−3.0	$9_{4,5} \leftarrow 9_{3,7}$	624 893.7	1.9
$6_{2,4} \leftarrow 6_{1,6}$	606 918.1	1.2	$14_{4,10} \leftarrow 14_{3,12}$	629 170.1	−1.3
$7_{2,5} \leftarrow 7_{1,7}$	610 530.1	−1.2	$14_{4,11} \leftarrow 13_{3,11}$	690 420.9	1.2
$5_{2,4} \leftarrow 4_{1,4}$	623 956.1	−4.1	$4_{4,0} \leftarrow 5_{5,0}$	502 619.8	1.9
$9_{2,8} \leftarrow 10_{3,8}$	502 617.9	−0.5	$4_{4,1} \leftarrow 5_{5,1}$	502 619.8	1.9
$9_{2,7} \leftarrow 10_{3,7}$	508 300.7	−1.6	$5_{4,2} \leftarrow 6_{5,2}$	498 303.9	1.0
$8_{2,7} \leftarrow 9_{3,7}$	507 700.0	−0.7	$5_{4,1} \leftarrow 6_{5,1}$	498 303.9	0.7
$8_{2,6} \leftarrow 9_{3,6}$	511 850.9	−1.3	$5_{5,1} \leftarrow 4_{4,1}$	659 585.7	0.9
$7_{2,6} \leftarrow 8_{3,6}$	512 616.5	−0.5	$6_{5,2} \leftarrow 5_{4,2}$	664 212.5	0.5
$7_{2,5} \leftarrow 8_{3,5}$	515 410.1	−1.4	$12_{5,7} \leftarrow 11_{4,7}$	691 895.2	0.9
$6_{2,5} \leftarrow 7_{3,5}$	517 385.6	−1.1	$12_{5,8} \leftarrow 11_{4,8}$	692 164.1	0.7
$6_{2,4} \leftarrow 7_{3,4}$	519 086.8	−1.4	$13_{5,8} \leftarrow 12_{4,8}$	696 324.2	4.1
$5_{2,4} \leftarrow 6_{3,4}$	522 030.5	−3.8	$13_{5,9} \leftarrow 12_{4,9}$	696 846.7	6.5
$3_{2,2} \leftarrow 4_{3,2}$	531 077.1	0.1	$14_{5,9} \leftarrow 13_{4,10}$	700 594.7	−3.3
$3_{2,1} \leftarrow 4_{3,1}$	531 219.2	0.2	$14_{5,10} \leftarrow 13_{4,10}$	701 537.8	−1.3
$2_{2,1} \leftarrow 3_{3,1}$	535 531.7	0.8	$6_{5,2} \leftarrow 6_{6,0}$	513 372.0	−1.0
$2_{2,0} \leftarrow 3_{3,0}$	535 560.5	0.5	$6_{5,1} \leftarrow 6_{6,1}$	513 372.0	−1.0
$7_{2,6} \leftarrow 7_{3,4}$	548 352.7	0.1	$7_{5,3} \leftarrow 7_{6,1}$	513 645.4	1.3
$6_{2,5} \leftarrow 6_{3,3}$	548 775.5	−0.1	$7_{5,2} \leftarrow 7_{6,2}$	513 645.4	1.3
$5_{2,4} \leftarrow 5_{3,2}$	548 975.9	−3.4	$8_{5,4} \leftarrow 8_{6,2}$	513 956.3	−0.9
$4_{2,3} \leftarrow 4_{3,1}$	549 045.1	1.2	$8_{5,3} \leftarrow 8_{6,3}$	513 956.3	−1.2
$3_{2,2} \leftarrow 3_{3,0}$	549 031.2	0.3	$8_{6,2} \leftarrow 9_{5,4}$	610 186.4	6.2
$3_{2,1} \leftarrow 3_{3,1}$	549 184.7	0.5	$8_{6,3} \leftarrow 9_{5,5}$	610 186.4	4.8
$4_{2,2} \leftarrow 4_{3,2}$	549 505.2	0.9	$11_{6,5} \leftarrow 11_{5,7}$	651 104.2	−2.3
$5_{2,3} \leftarrow 5_{3,3}$	550 045.1	−2.7	$10_{6,4} \leftarrow 10_{5,6}$	650 930.2	−2.6
$6_{2,4} \leftarrow 6_{3,4}$	550 882.3	−0.7	$9_{6,4} \leftarrow 9_{5,4}$	650 748.8	−1.8
$7_{2,5} \leftarrow 7_{3,5}$	552 057.4	−0.8	$8_{6,2} \leftarrow 8_{5,4}$	650 574.2	3.9
$8_{2,6} \leftarrow 8_{3,6}$	553 590.6	−0.6	$8_{6,3} \leftarrow 8_{5,3}$	650 574.2	4.3
$10_{2,8} \leftarrow 10_{3,8}$	557 662.6	0.4	$7_{6,1} \leftarrow 7_{5,3}$	600 387.8	−5.5
$9_{2,7} \leftarrow 8_{3,5}$	595 380.3	0.4	$7_{6,2} \leftarrow 7_{5,2}$	600 387.8	−5.4
$11_{2,9} \leftarrow 10_{3,7}$	607 453.7	4.8	$7_{6,1} \leftarrow 6_{5,1}$	681 756.1	−4.7
$12_{2,10} \leftarrow 11_{3,8}$	613 135.7	0.9	$7_{6,2} \leftarrow 6_{5,2}$	681 756.1	−4.8
$6_{3,4} \leftarrow 7_{2,6}$	581 258.1	0.3	$8_{6,2} \leftarrow 7_{5,2}$	686 447.8	4.4
$13_{3,10} \leftarrow 13_{2,12}$	629 180.0	−1.0	$8_{6,3} \leftarrow 7_{5,3}$	686 447.8	4.3
$11_{3,8} \leftarrow 11_{2,10}$	620 927.6	0.0	$9_{6,4} \leftarrow 8_{5,4}$	691 139.7	−1.1
$9_{3,6} \leftarrow 9_{2,8}$	615 872.7	2.6	$10_{7,3} \leftarrow 10_{6,5}$	664 067.7	1.6
$8_{3,5} \leftarrow 8_{2,7}$	614 284.9	1.0	$7_{7,0} \leftarrow 6_{6,0}$	694 657.3	5.5
$8_{3,6} \leftarrow 8_{2,6}$	607 772.7	2.6	$7_{7,1} \leftarrow 6_{6,1}$	694 657.3	5.5
$7_{3,4} \leftarrow 7_{2,6}$	613 163.7	0.6	$8_{7,1} \leftarrow 7_{6,1}$	699 361.7	−1.2
$6_{3,3} \leftarrow 6_{2,5}$	612 395.9	−1.3	$10_{7,3} \leftarrow 9_{6,3}$	708 850.3	3.0
$5_{3,3} \leftarrow 5_{2,3}$	610 687.6	−3.8	$10_{7,4} \leftarrow 9_{6,4}$	708 850.3	3.0
$4_{3,1} \leftarrow 4_{2,3}$	611 578.8	1.2	$11_{7,5} \leftarrow 10_{6,5}$	713 613.4	0.4
$3_{3,0} \leftarrow 3_{2,2}$	611 387.1	−0.4	$12_{7,5} \leftarrow 11_{6,5}$	718 388.8	0.9
$5_{3,3} \leftarrow 4_{2,3}$	634 152.0	−4.8	$12_{7,6} \leftarrow 11_{6,6}$	718 388.8	0.7
$13_{3,10} \leftarrow 12_{2,10}$	665 510.5	−0.5	$8_{8,0} \leftarrow 7_{7,0}$	712 218.9	−1.0

Table 2
Spectroscopic constants for the combined fit of the *ortho*-state of the propane water dimer.

State		Steyert et al. [14]	New fit
Ground state	A/MHz	8443.24 (12)	8442.160 (57)
	B/MHz	2507.6611 (22)	2507.6622 (14)
	C/MHz	1969.3165 (22)	1969.3159 (17)
	D_J/kHz	10.203 (78)	10.173 (30)
	D_{JK}/kHz	211.44 (50)	212.14 (24)
	D_K/kHz	0.0[a]	−212.3 (38)
	d_1/kHz	4.166 (46)	−4.188 (25)
	d_2/kHz	8.68 (49)	−0.933 (20)
	H_J/kHz	0.00023 (18)	0.00035 (35)
	H_{JK}/kHz	0.0095 (23)	0.0389 (50)
	H_{KJ}/kHz	−1.26 (12)	−0.976 (24)
	H_K/kHz	−15.1 (22)	0.488 (58)
Excited state	E/MHz	579,691.20 (24)	579,690.38 (32)
	cm^{-1}	19.336417 (8)	19.336390 (11)
	A/MHz	8512.765 (61)	8513.112 (49)
	B/MHz	2503.631 (18)	2503.614 (20)
	C/MHz	1997.940 (18)	1997.983 (24)
	D_J/kHz	12.009 (61)	12.02 (19)
	D_{JK}/kHz	87.0 (12)	89.12 (94)
	D_K/kHz	51.0 (28)	164.09 (89)
	d_1/kHz	3.348 (94)	−3.118 (86)
	d_2/kHz	−0.875 (29)	−0.923 (32)
	H_J/kHz	0.0[a]	−1.90 (70)
	H_{JK}/kHz	−0.0216 (74)	−0.0204 (46)
	H_{KJ}/kHz	−0.027 (25)	0.0[a]
	H_K/kHz	10.539 (25)	0.0[a]
	N	155	299
	σ/MHz	1.1	1.6

[a] Value within one standard deviation of zero, fixed at zero for this fit.

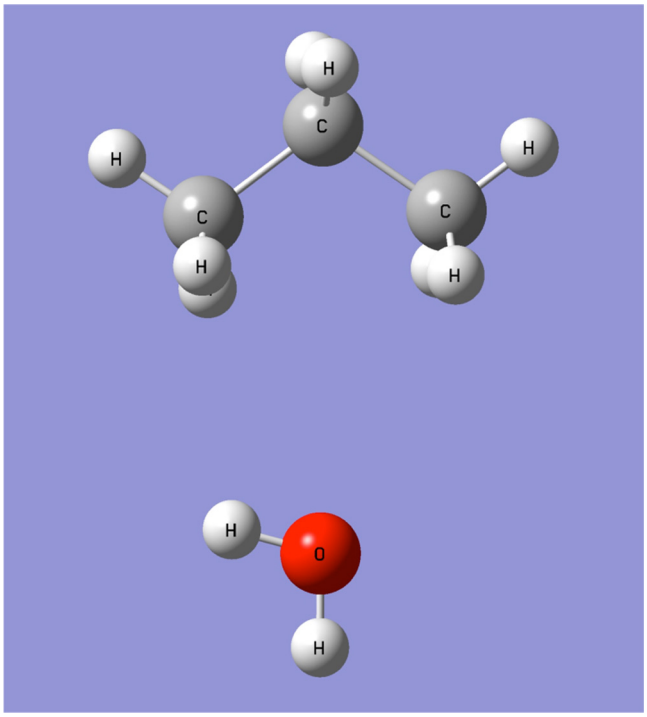

Figure 2. One of the proposed equilibrium structures for the propane–water dimer [13] based on the projection of dipole moment of water, wherein the oxygen atom sits on the C_2 axis of propane monomer and all three atoms of water remain in the plane of the carbon atoms of propane.

the *a* inertial axis of the dimer is approximately aligned with the *b* inertial axis of the free propane molecule. This would be true if propane were forming a dimer with a rare gas atom like argon or neon [20]. However, in the case of the propane–water dimer, water is of a structure that will contribute at least somewhat to I_a. If we assume a rigid structure for the dimer such that the center of mass of water lies on the *b* inertial axis of the free propane molecule, we can rationalize a value for the *A* rotational constant of 8330 MHz. Ref. [13] considered a scenario wherein the center of mass of water is slightly displaced from the *b* inertial axis of the propane molecule, but concluded that it would rapidly decrease *A*, while increasing the *C* rotational constant. A possible explanation for this is the large amplitude motions of the water molecule. As observed for the ammonia dimer [21–23] and argon–water dimer [24], a large amplitude motion of similar timescale can exhibit significant mixing with *A* axis rotation and other internal motions. The proposed structure for the propane–water dimer is shown in Figure 2.

We assigned this torsional band of the propane–water dimer comprising all of the *P*-, *Q*-, and *R*-branches using a semi-rigid rotor Hamiltonian and obtained the new information given in Table 2, including refined values for the rotational constants and band origin, but this single VRT band does not allow a definite vibrational assignment. After the assignment of the additional transitions described above, there remain about three hundred unassigned transitions between 680 GHz and 810 GHz. It is possible that these transitions belong to either the *para*-state of the propane–water dimer or larger propane water clusters, or perhaps to a VRT state of the argon–propane dimer. Extensive continuous spectral coverage at higher frequency is needed in order to make further progress on assigning these transitions, and alternative technology is currently being explored to effect such additional study [25].

Acknowledgements

This work was supported by Experimental Physical Chemistry Division of the National Science Foundation under Grant No. 1300723 for RJS. This work was supported in part by the U.S. Department of Energy, Office of Science, Office of Workforce Development for Teachers and Scientists (WDTS) under the Visiting Faculty Program (VFP). WL thanks the Welch Foundation for financial support.

References

[1] R. Kleinberg, P. Brewer, Am. Sci. 89 (2001) 244.
[2] K. Lambeck, T.M. Esat, E.-K. Potter, Nature 419 (2002) 199.
[3] H. Lu, et al., Nature 445 (2007) 303.
[4] C. Leforestier, F. Gatti, R.S. Fellers, R.J. Saykally, J. Chem. Phys. 117 (2002) 8710.
[5] R. Bukowski, K. Szalewicz, G.C. Groenenboom, A. van der Avoird, Science 315 (2007) 1249.
[6] F.N. Keutsch, R.J. Saykally, Proc. Natl. Acad. Sci. U. S. A. 98 (2001) 10533.
[7] D. Chandler, Nature 437 (2005) 640.
[8] L. Dore, R.C. Cohen, C.A. Schmuttenmaer, K.L. Busarow, M.J. Elrod, J.G. Loeser, R.J. Saykally, J. Chem. Phys. 100 (1994) 863.
[9] R.D. Suenram, G.T. Fraser, F.J. Lovas, Y. Yawashima, J. Chem. Phys. 101 (1994) 7230.
[10] K.L. Copeland, G.S. Tschumper, J. Chem. Theory Comput. 8 (2012) 1646.
[11] Z. Cao, J.W. Tester, B.L. Trout, J. Chem. Phys. 115 (2001) 2550.
[12] J.B.L. Martins, J.R.S. Politi, E. Garcia, A.F.A. Vilela, R. Gargano, J. Phys. Chem. A 113 (2009) 14818.
[13] D.W. Steyert, M.J. Elrod, R.J. Saykally, F.J. Lovas, R.D. Suenram, J. Chem. Phys. 99 (1993) 7424.
[14] D.W. Steyert, M.J. Elrod, R.J. Saykally, J. Chem. Phys. 99 (1993) 7431.
[15] R.J. Saykally, Acc. Chem. Rev. 22 (1989) 295.
[16] R.C. Cohen, R.J. Saykally, J. Phys. Chem. 96 (1992) 1024.
[17] H.M. Pickett, J. Mol. Spectrosc. 148 (1991) 371.
The SPCAT and SPFIT spectroscopic predicting and fitting programs are available as free downloads from http://spec.jpl.nasa.gov/
[18] D.W. Steyert, (Ph.D. Thesis) University of California at Berkeley.
[19] D.R. Lide, J. Chem. Phys. 33 (1960) 1514.
[20] K.I. Peterson, D. Pullman, W. Lin, A.J. Minei, S.E. Novick, J. Chem. Phys. 127 (2007) 184306.
[21] J.G. Loeser, et al., J. Chem. Phys. 97 (1992) 4727.

[22] W. Lin, J.-X. Han, L.K. Takahashi, J.G. Loeser, R.J. Saykally, J. Phys. Chem. A 110 (2006) 8011.
[23] W. Lin, J.-X. Han, L.K. Takahashi, J.G. Loeser, R.J. Saykally, J. Phys. Chem. A 111 (2007) 9680.
[24] R.C. Cohen, K.L. Busarow, K.B. Laughlin, G.A. Blake, M. Havenith, Y.T. Lee, R.J. Saykally, J. Chem. Phys. 89 (1988) 4494.
[25] I. Mehdi, E. Schlecht, G. Chattopadhyay, P.H. Siegel, Proc. SPIE 4855 (2003) 435.